JOC The Journal of Organic Chemistry

Article

pubs.acs.org/joc

Theoretical Study of Mechanism and Stereoselectivity of Catalytic Kinugasa Reaction

Stefano Santoro,† Rong-Zhen Liao, Tommaso Marcelli, Peter Hammar, and Fahmi Himo*

Department of Organic Chemistry, Arrhenius Laboratory, Stockholm University, SE-106 91 Stockholm, Sweden

Supporting Information

ABSTRACT: The mechanism of the catalytic Kinugasa reaction is investigated by means of density functional theory calculations. Different possible mechanistic scenarios are presented using phenanthroline as a ligand, and it is shown that the most reasonable one in terms of energy barriers involves two copper ions. The reaction starts with the formation of a dicopper-acetylide that undergoes a stepwise cycloaddition with the nitrone, generating a five-membered ring intermediate. Protonation of the nitrogen of the metalated isoxazoline intermediate results in ring opening and the formation of a ketene intermediate. This then undergoes a copper-catalyzed cyclization by an intramolecular nucleophilic attack of the nitrogen on the ketene, affording a cyclic copper enolate. Catalyst release and tautomerization gives the final β-lactamic product. A comprehensive study of the enantioselective reaction was also performed with a chiral bis(azaferrocene) ligand. In this case, two different reaction mechanisms, involving either the scenario with the two copper ions or a direct cycloaddition of the parent alkyne using one copper ion, were found to have quite similar barriers. Both mechanisms reproduced the experimental enantioselectivity, and the current calculations can therefore not distinguish between the two possibilities.

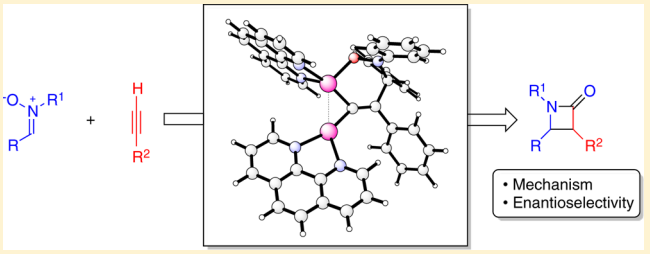

1. INTRODUCTION

β-Lactams stand among the most significant heterocyclic cores in pharmaceutical chemistry.[1] Drugs belonging to the penicillin, cephalosporin and carbapenem families are extensively used for treatment of several conditions due to their broad-spectrum of antibacterial activity. In antibiotics, the β-lactam core typically contains two trisubstituted chiral carbons, which can have either *syn* or *anti* relative stereochemistry. Besides their interest as end-compounds, enantiopure β-lactams are useful synthons, which can be readily manipulated to yield β-amino acids and azetidines.[2] It is therefore not surprising that considerable synthetic efforts have been devoted to the development of reliable methods for the stereoselective synthesis of functionalized β-lactams. In this respect, the most general entry to disubstituted β-lactams is probably represented by Staudinger's [2 + 2] ketene/imine cycloaddition (Scheme 1a).[3] Until the late 1990s, all the asymmetric versions of this reaction involved the use of chiral auxiliaries. The intense research efforts of the past decade resulted in several protocols for the catalytic asymmetric synthesis of β-lactams using a variety of chiral promoters including chiral organic bases, chiral Lewis acids, and combinations thereof.[3]

A less-explored approach to the synthesis of β-lactams involves the Cu(I)-catalyzed reaction of nitrones with alkynes, also known as the Kinugasa reaction (Scheme 1b).[4] This mostly leads to the formation of *cis*-lactams although the diastereoselectivity is strongly dependent on the experimental conditions.[4b] Conceptually, this transformation is by no means less appealing than the Staudinger reaction. In fact, also the

Scheme 1. Synthesis of β-Lactams: (a) the Staudinger and (b) the Kinugasa Reactions

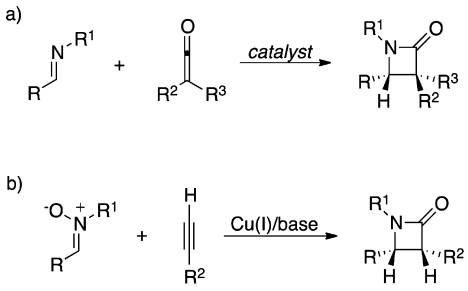

Kinugasa reaction has optimal atom economy and proceeds with complete regioselectivity. First reported in 1972 using preformed Cu(I)-acetylides,[5] the Kinugasa reaction was rendered catalytic in copper 20 years later by Miura et al.[6] The first highly enantioselective catalytic version of this reaction was reported by Fu and co-workers, who obtained up to 93% ee in the reaction of *N*-aryl nitrones with different alkynes using bis(azaferrocene) ligands (Scheme 2).[7] Later, this protocol was extended to an intramolecular version of this reaction.[8] Following these studies, other chiral catalysts have been applied in the enantioselective Kinugasa reaction with variable degrees of success.[9]

Received: December 16, 2014
Published: February 5, 2015

DOI: 10.1021/jo502838p
J. Org. Chem. 2015, 80, 2649−2660

Scheme 2. Enantioselective Version of the Kinugasa Reaction[7]

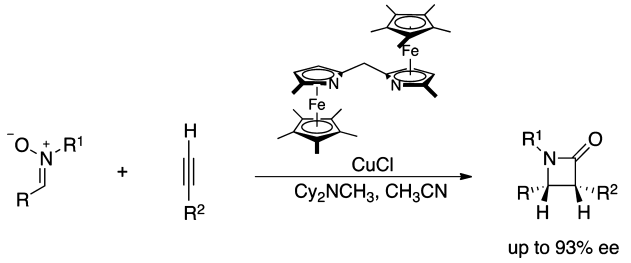

The mechanism of the Kinugasa reaction is still not satisfactorily understood. Two mechanistic proposals are present in the literature (Scheme 3). In both cases, the initial steps involve the formation of Cu(I)-acetylide followed by a cycloaddition leading to a metalated isoxazoline intermediate. The two proposals differ mainly in the mechanism of the formal ring contraction from the isoxazoline intermediate to form the β-lactam. Ding and Irwin have proposed a mechanism involving the formation of a bicyclic intermediate made by an azetidine fused with an oxaziridine (Scheme 3a).[10]

DeShong and co-workers reported a modification of the Kinugasa reaction involving a thermal [3 + 2] cycloaddition of silylacetylides and nitrones followed by desilylation with fluoride.[11] In this case, it was suggested that the ring opening triggered by desilylation would yield a highly reactive imidoketene intermediate that immediately undergoes ring closure to form a β-lactam enolate. On the basis of this proposal, a possible alternative for the mechanism of the Kinugasa reaction has been suggested, involving the opening of the isoxazoline ring and the formation of a ketene intermediate (Scheme 3b).[4b,8,9d] This mechanistic proposal is consistent with findings by Shintani and Fu, who were able to trap the enolate intermediate with an electrophile other than proton, namely, allyl iodide. In this case, it was proposed that, after expulsion from the isoxazoline intermediate, Cu(I) would bind to the oxygen of the lactam enolate.[8]

In spite of the considerable developments of recent years, there is still large room for improvements to turn the Kinugasa reaction into a highly efficient synthetic tool. To this end, a detailed mechanistic understanding of this reaction will be crucial to further advance its scope and applications by rational design of new and improved catalytic systems. Here, we present a density functional theory (DFT) study of the reaction mechanism and enantioselectivity of the catalytic Kinugasa reaction reported by Fu and co-workers (Scheme 2).[7] To do this, we first performed a detailed investigation of the reaction under the same conditions but with a smaller nonchiral ligand (phenanthroline) in order to work out and compare various mechanistic possibilities.

2. COMPUTATIONAL METHODS

All calculations were carried out using density functional theory with the B3LYP functional,[12] as implemented in the Gaussian03 program package.[13] For geometry optimizations, the 6-31G(*d,p*) basis set was used for the C, N, O, H elements, and the LANL2DZ[14] pseudopotential for Cu and Fe. On the basis of these optimized geometries, single-point calculations were carried out with the 6-311+G(*2d,2p*) basis set for all elements. The stationary points were confirmed as minima (no imaginary frequencies) or transition states (only one imaginary frequency) by analytical frequency calculations at the same theory level as the geometry optimizations. Selected reaction pathways were subjected to intrinsic reaction coordinate (IRC)[15] analysis in order to trace their paths and to confirm that the optimized transition state (TS) structures connect the correct reactants and products. The reported energies are Gibbs free energies, which include zero-point vibrational corrections, thermal and entropy corrections at 298 K and solvation energies. The latter are calculated as single-point corrections on the optimized structures with the same basis set combination used for the geometry optimizations, using the conductor-like polarizable continuum model (CPCM)[16] method with the UAKS radii and with the parameters for acetonitrile, according to the experimental procedure by Fu and co-workers.[7] On the basis of the optimized geometries, all energies were also corrected with single-point dispersion effects using the DFT-D2 method of Grimme,[17] as recent reports have shown that inclusion of these effects can significantly improve the accuracy of the B3LYP method.[18]

3. RESULTS AND DISCUSSION

3.1. Uncatalyzed Cycloaddition Reaction. For comparison, we first consider the uncatalyzed reaction between *N*,α-diphenyl nitrone **1** and phenyl acetylene **2** (Figure 1). The 1,3-dipolar cycloaddition can occur with two different orientations, leading to two regioisomeric adducts. Only one of these (**INT-U1**) can however react further leading eventually to the β-lactam, while the other isomer (**INT-U2**) has the wrong connectivity. The 1,3-dipolar cycloaddition leading to the potentially productive intermediate has a barrier of 29.6 kcal/mol, and the reaction is exergonic by 20.8 kcal/mol. The reaction leading to

Scheme 3. Previously Proposed Reaction Mechanisms[10,4b,8,9d]

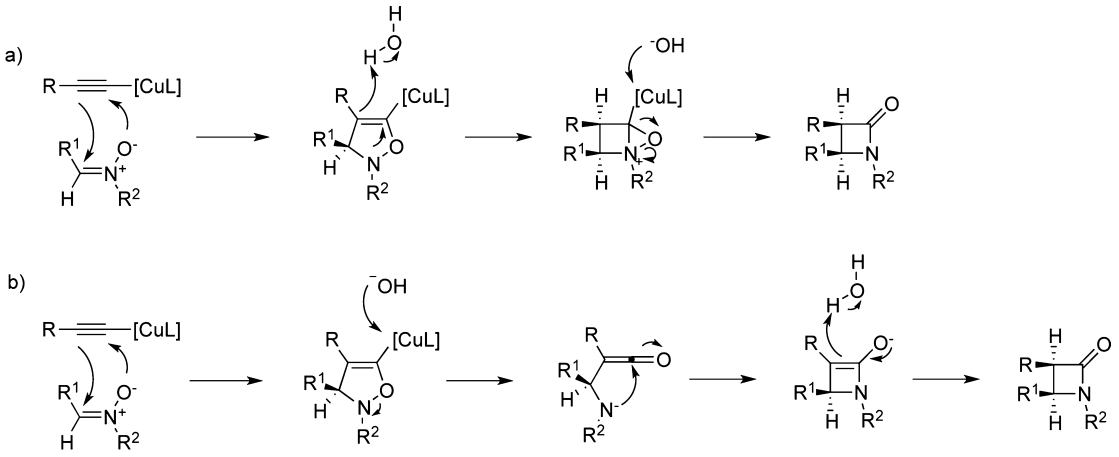

DOI: 10.1021/jo502838p
J. Org. Chem. 2015, 80, 2649−2660

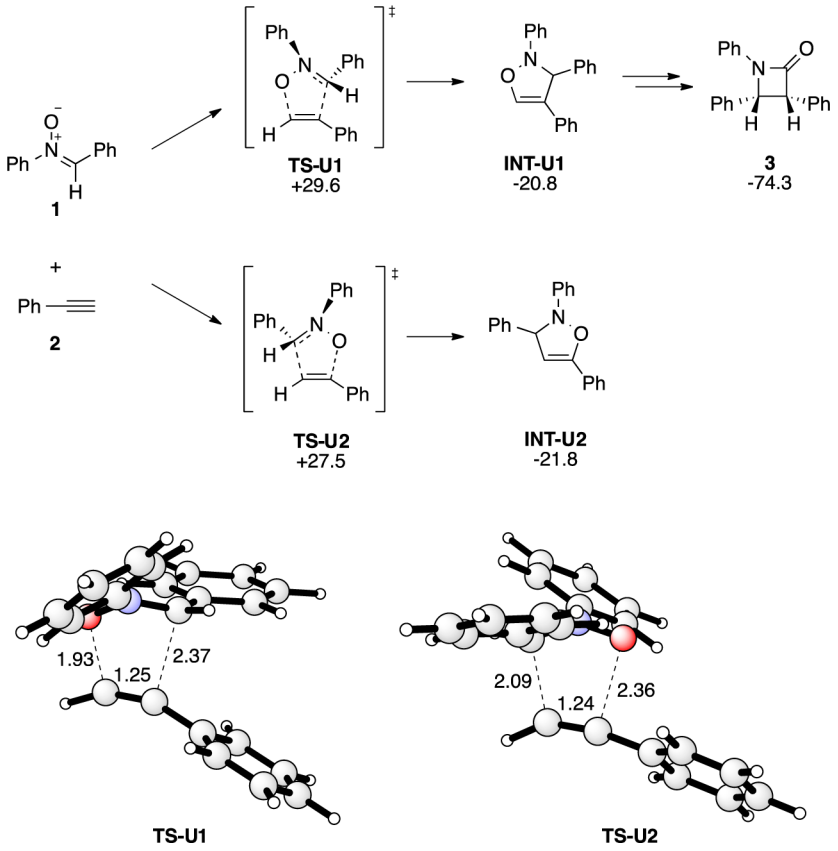

Figure 1. Uncatalyzed cycloaddition reaction. Energies are in kilocalories per mole (kcal/mol), distances in ångströms (Å).

intermediate **INT-U2**, which cannot react further to afford the *β*-lactam, has a lower barrier (27.5 kcal/mol) and is exergonic by 21.8 kcal/mol. The formation of the final product **3** starting from the alkyne and the nitrone is exergonic by as much as 74.3 kcal/mol. These results will be useful when establishing the mechanism of the catalytic reaction below. For example, the overall barriers of the Cu-catalyzed reaction should be lower than the uncatalyzed one and the catalyst should lower the barrier for the productive pathway more than the unproductive one.

3.2. Nonchiral Reaction with Phenanthroline Ligand.

In this section, we investigate the full catalytic cycle with a nonchiral ligand, before studying the origins of the enantioselectivity in Fu's system[7] in the next section. Here, phenanthroline is used as the copper ligand, because it might be considered as a good model of the electronic structure of the chiral catalyst, and it was also one of the ligands used by Miura and co-workers.[6]

Both mechanisms proposed previously assume that the first step of the reaction is the deprotonation of the alkyne to give a copper-acetylide (Scheme 3). Although coordination to copper acidifies the acetylene considerably,[19] the calculations show that this deprotonation, using triethylamine as a base in acetonitrile solution (in accordance with the reaction conditions used by Fu and co-workers),[20] is endergonic by 9.2 kcal/mol (eq 1). This value is not too high to be overcome, but it has to be taken into account in the analysis of the overall free energy profile, as will be discussed below.

Quite recently, there have been both experimental and theoretical evidence suggesting the involvement of two copper species in the mechanism of the Cu(I)-catalyzed azide−alkyne cycloaddition (CuAAC).[21] Due to the similarities between the CuAAC reaction and the cycloaddition implicated in the Kinugasa reaction, we have tested this possibility also here. Results show that the deprotonation of phenylacetylene **2** using two copper-phenanthroline complexes to afford intermediate **B** now is exergonic by 3.3 kcal/mol (eq 2). It is thus 12.5 kcal/mol more favorable to deprotonate the acetylene in the presence of two copper ions compared to only one.[22]

In intermediate **B**, the alkynyl ligand is *σ*-bound to one copper ion, with the other copper coordinating the *π*-system (see optimized geometry in Figure 3). We could also locate

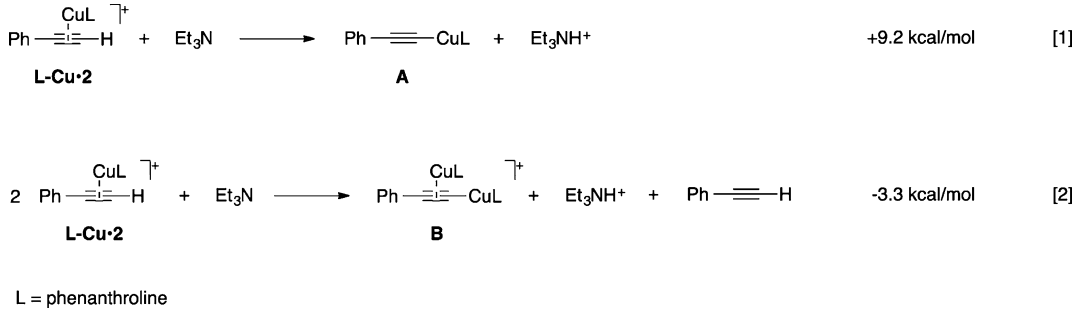

DOI: 10.1021/jo502838p
J. Org. Chem. 2015, 80, 2649−2660

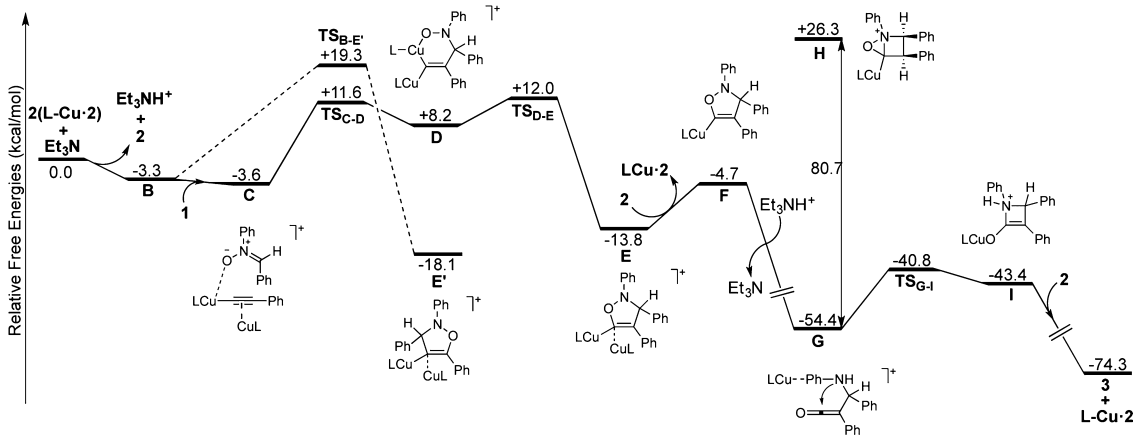

Figure 2. Calculated free energy profile for the reaction mechanism with phenanthroline ligand involving the deprotonation of the alkyne in the presence of two copper ions as the initial step.

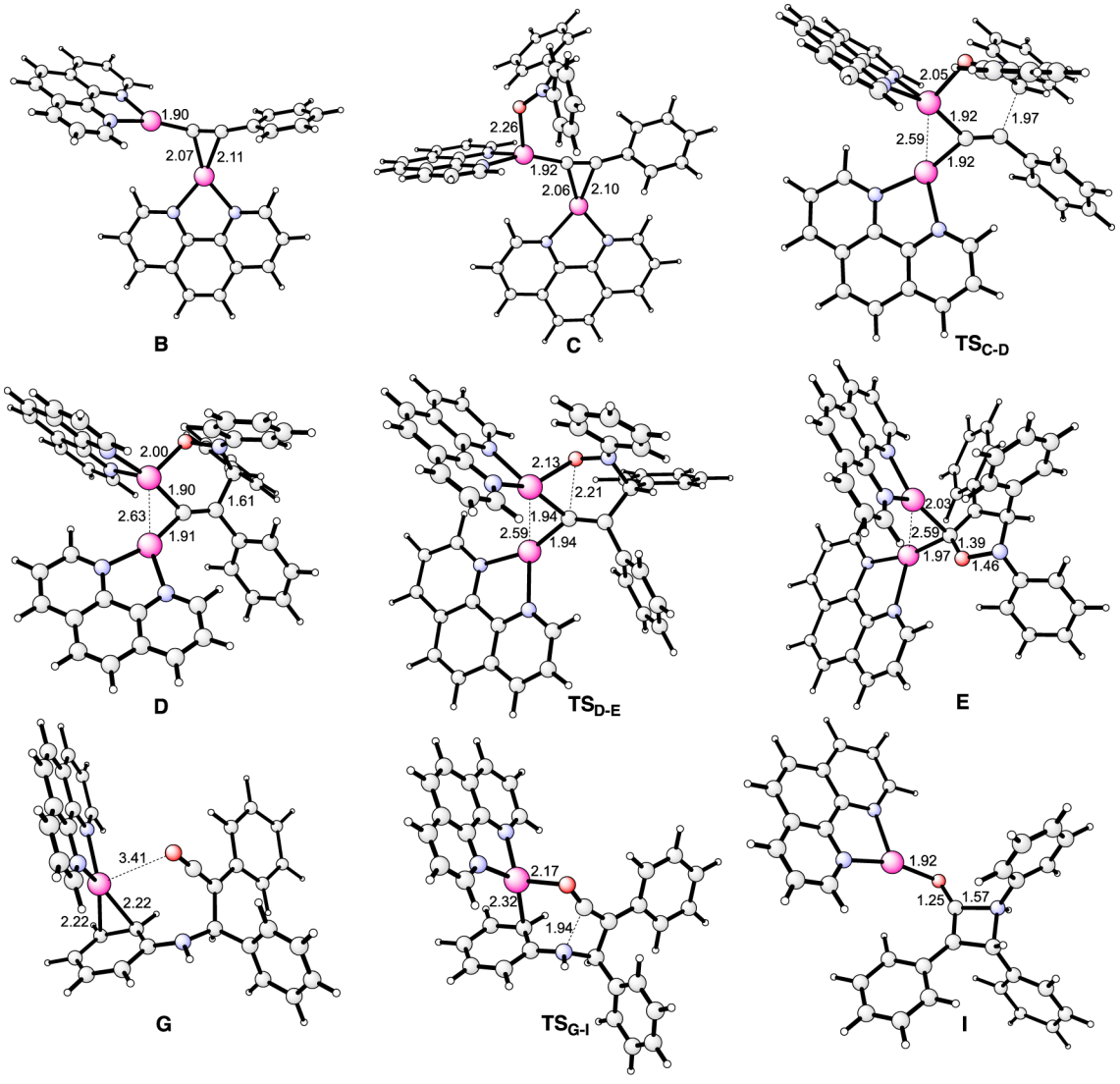

Figure 3. Optimized structures of selected stationary points for the mechanism with phenanthroline ligand involving the deprotonation of the alkyne in the presence of two copper atoms as the initial step.

an alternative complex in which the alkynyl ligand is bridging the two metals in a strict μ^2-mode, but this was found to be 2.5 kcal/mol higher in energy than **B** (see Supporting Information). The geometry of **B** resembles those previously reported for related systems in the CuAAC reaction,[21d] with the exception that in **B** the π-coordinated copper ion is almost equidistant from the two alkyne carbons, rather than significantly closer to the terminal one.[21d]

DOI: 10.1021/jo502838p
J. Org. Chem. 2015, 80, 2649−2660

Scheme 4. Suggested Mechanism with Phenanthroline Ligand Based on the Present Calculations Involving the Deprotonation of the Alkyne in the Presence of Two Copper Ions as the Initial Step

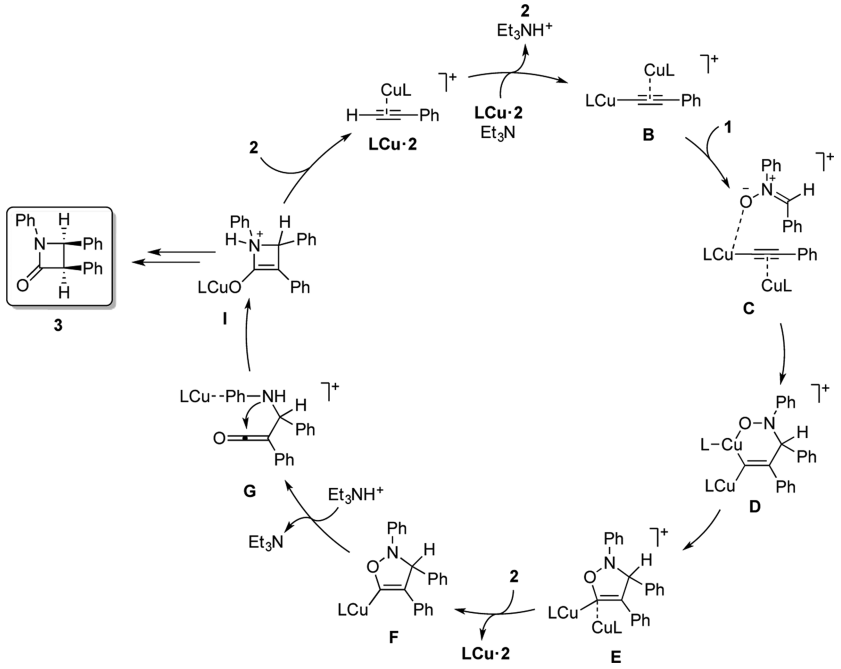

In light of these findings regarding the alkyne deprotonation, we decided to investigate the reaction mechanism with either two or one copper complexes assisting the cycloaddition. The reaction involving two copper ions demonstrated significantly better overall energetics and will therefore be discussed first.

The reaction starts by the coordination of the oxygen of nitrone **1** to one of the copper ions of **B** to give intermediate **C**. The coordination is, however, very weak, since the energy gain is only 0.3 kcal/mol (see Figure 2). The following formal cycloaddition occurs then in a stepwise fashion. The first step involves a carbon−carbon bond formation ($\mathbf{TS_{C\text{-}D}}$), leading to the six-membered ring intermediate **D**, in which one of the coppers is formally Cu(III) (see Figure 3 for optimized structure). This step has a barrier of 15.2 kcal/mol and is endergonic by 11.8 kcal/mol relative to **C**. The formation of the five-membered ring intermediate **E** occurs then through transition state $\mathbf{TS_{D\text{-}E}}$, which can be seen as a formal reductive elimination affording a Cu(I) species again. The overall barrier leading to intermediate **E** is 15.6 kcal/mol relative to **C**, and the process is exergonic by 13.8 kcal/mol, relative to the isolated reactants (see Figure 2).

At this stage, we also investigated whether concerted cycloadditions, similar to the uncatalyzed ones, were possible as alternatives to the stepwise cycloaddition. We could locate a transition state ($\mathbf{TS_{B\text{-}E'}}$) for the concerted cycloaddition occurring on intermediate **B** with the nonproductive regiochemistry (analogous to **TS-U2**, Figure 1). The barrier for this reaction is, however, 7.3 kcal/mol higher than the one calculated for the stepwise pathway. Furthermore, every attempt to optimize a transition state for the cycloaddition occurring with the productive regiochemistry, which should lead to the formation of intermediate **E**, converged to the stepwise pathway.

From **E**, the calculations show that, after decoordination of one of the copper moieties, protonation of the nitrogen of isoxazoline **F** leads directly to the ring opening and the formation of ketene intermediate **G**. The decoordination of LCu^+ (with the assistance of one alkyne molecule, i.e., from **E** to **F** in Figure 2) is endergonic by 9.1 kcal/mol, but the subsequent nitrogen protonation by Et_3NH^+ and the concomitant ring-opening step is highly exergonic, by ca. 50 kcal/mol relative to **F**. The alternative direct protonation of the nitrogen in intermediate **E** does not lead to ring opening, and affords a dicationic intermediate that is 6.1 kcal/mol higher in energy than intermediate **F**. Thus, it is more likely that the decoordination of one of the copper ions precedes the protonation of the nitrogen.

Here, the energy of intermediate **G** can be compared directly to the energy of the bicyclic intermediate **H** proposed by Ding and Irwin (Scheme 3).[10] The calculations show that this bicyclic intermediate is 31 kcal/mol higher in energy than **F**, and as much as 80 kcal/mol higher than ketene **G**, arguably due to the high strain of the rings. This finding is thus sufficient to rule out the involvement of this intermediate in the reaction mechanism.

From intermediate **G**, the formation of the final four-membered ring can occur through a nucleophilic attack of the nitrogen on the ketene. We found that this nucleophilic attack/cyclization, occurring through $\mathbf{TS_{G\text{-}I}}$, has a quite low barrier (13.6 kcal/mol). In $\mathbf{TS_{G\text{-}I}}$, the metal shifts from the nitrogen-bound phenyl group to the carbonyl oxygen (Figure 3). Thus, the copper assists this cyclization, by acting as a Lewis acid on the ketene carbonyl, and stabilizing the resulting enolate.[23]

From intermediate **I**, the release of the copper catalyst and a tautomeric equilibrium are necessary for the completion of the catalytic cycle. This step was found to be exergonic by 30.9 kcal/mol. The protonation of the cyclic enolate determines which diastereoisomer is formed. It is thus expected that protonation from the least sterically hindered face is responsible for the formation of the *cis*-product.

The obtained mechanism involving two copper ions is summarized in Scheme 4. The copper-catalyst is involved in each step of the reaction, effectively lowering the energy barriers for all of them. First, copper coordination increases the acidity of the terminal alkyne, facilitating its deprotonation by a relatively weak base such as a tertiary amine. As discussed above, the involvement of a second copper ion in this step

DOI: 10.1021/jo502838p
J. Org. Chem. 2015, 80, 2649−2660

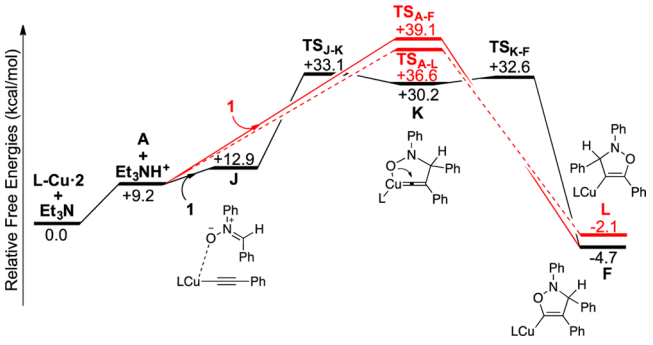

Figure 4. Free energy profile for the reaction mechanisms with phenanthroline ligand involving the deprotonation of the alkyne in the presence of one copper ion as the initial step.

makes the deprotonation significantly easier. Second, copper allows the cycloaddition to occur in a stepwise fashion, with much lower energy barriers compared to those found for the uncatalyzed reaction (15.6 vs 27.5 kcal/mol). Finally, copper acts as a Lewis acid in promoting the nucleophilic attack of the nitrogen on the ketene ($\mathbf{TS_{G\text{-}I}}$) and stabilizing the resulting enolate (**I**).

As discussed above, we also considered a possible reaction mechanism involving only one copper ion. The calculated free energy profile for this scenario is shown in Figure 4, while the optimized structures are provided in Supporting Information. In this case, we could locate the transition states for the cycloaddition in both concerted and stepwise manners. The stepwise pathway is very similar to the one found for the reaction involving two coppers (cf. Figures 2 and 3), with an initial C−C bond formation affording a six-membered ring intermediate (**K**), followed by a ring contraction leading to metalated isoxazoline **F**. In the concerted pathway, intermediate **F** is formed through $\mathbf{TS_{A\text{-}F}}$, an asynchronous transition state with a shorter distance for the forming C−C bond compared to the forming C−O bond (2.05 and 2.47 Å, respectively). We could also locate a transition state ($\mathbf{TS_{A\text{-}L}}$) for the concerted cycloaddition occurring with the opposite regiochemistry. This would lead to the formation of the nonproductive metalated isoxazoline **L**. However, all these possibilities turned out to have too high barriers to be viable under the experimental reaction conditions. The stepwise mechanism has a barrier of 33.1 kcal/mol ($\mathbf{TS_{J\text{-}K}}$), while the concerted one has barriers of 36.6 or 39.1 kcal/mol, depending on the regiochemistry of the cycloaddition. It is noteworthy that even without considering the initial alkyne deprotonation and the nitrone coordination (i.e., starting directly from **J**), the reaction catalyzed by one copper ion has higher barriers compared to the one involving two copper ions (20.2 vs 15.6 kcal/mol). However, the energy cost of the initial deprotonation of 9.2 kcal/mol has to be added and contributes significantly to raising the barriers for the mechanism involving only one copper ion.

Considering these results, we have also investigated possible mechanisms involving cycloaddition of the parent alkyne, i.e., without the initial deprotonation. Similarly to the above case, we located the transition states for the cycloaddition occurring in both stepwise and concerted manners (Figure 5 and Scheme 5, optimized structures are given in the Supporting information). In the stepwise mechanism, the copper initially coordinates both the alkyne and nitrone oxygen (**M**, Scheme 5). In the first step, the formation of a 6-membered ring intermediate (**N**), formally a Cu(III)-species, occurs through a cyclic carbocupration, while the second step is a formal reductive elimination ($\mathbf{TS_{N-O}}$, Figure 5). The calculated barrier for this scenario is 23.9 kcal/mol, which is reasonable but higher than those found for the mechanism involving two copper ions. In the concerted mechanism, copper catalyzes the addition of the nitrone on the alkyne by coordinating to its π-system, in a plane perpendicular to the direction of the attacking nitrone ($\mathbf{TS_{1+2\text{-}P}}$). This leads to an isoxazoline (**P**), that is the same as the one obtained through the stepwise mechanism (**O**) except for the position of the copper ion, which is on the C−C endocyclic double bond in **P** and coordinates the nitrogen-bound phenyl ring in **O**. The calculated energy barrier is very similar to the one found for the stepwise mechanism occurring through $\mathbf{TS_{M\text{-}N}}$ and $\mathbf{TS_{N-O}}$ (25.1 vs 23.9 kcal/mol).

To proceed from the isoxazoline intermediate, deprotonation of the carbon adjacent to the oxygen is necessary. We found that this deprotonation, when effected by the Et_3N base and with the copper coordinated to the endocyclic double bond, has a reasonable barrier of 22.9 kcal/mol (from **P** to $\mathbf{TS_{R\text{-}F'}}$). This step is endergonic by 15.6 kcal/mol, but it should be noted that the subsequent protonation of intermediate **F′** by Et_3NH^+, with the consequential ring opening leading to the formation of ketene **G**, is highly exergonic (ca. 50 kcal/mol).[24] After the formation of intermediate **G**, the mechanism is same as the previously considered one involving the initial formation of the dicopper-acetylide (Scheme 4).

It is important to note that the initial concerted cycloaddition can also occur with opposite regiochemistry through $\mathbf{TS_{1+2\text{-}Q}}$, affording the unproductive isoxazoline **Q**. The barrier for this

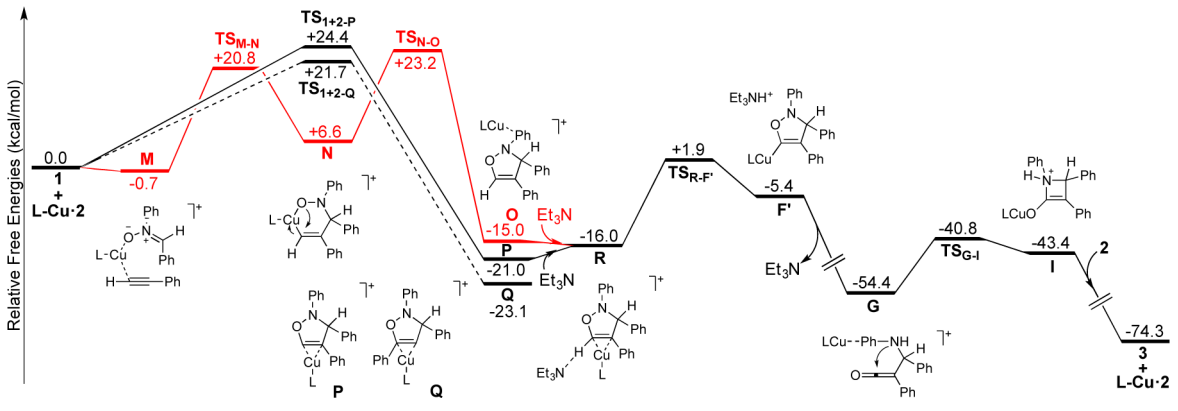

Figure 5. Free energy profile for the reaction mechanism with phenanthroline ligand without initial deprotonation of the alkyne.

DOI: 10.1021/jo502838p
J. Org. Chem. 2015, 80, 2649−2660

Scheme 5. Reaction Mechanism with Phenanthroline Ligand without Initial Deprotonation of the Alkyne

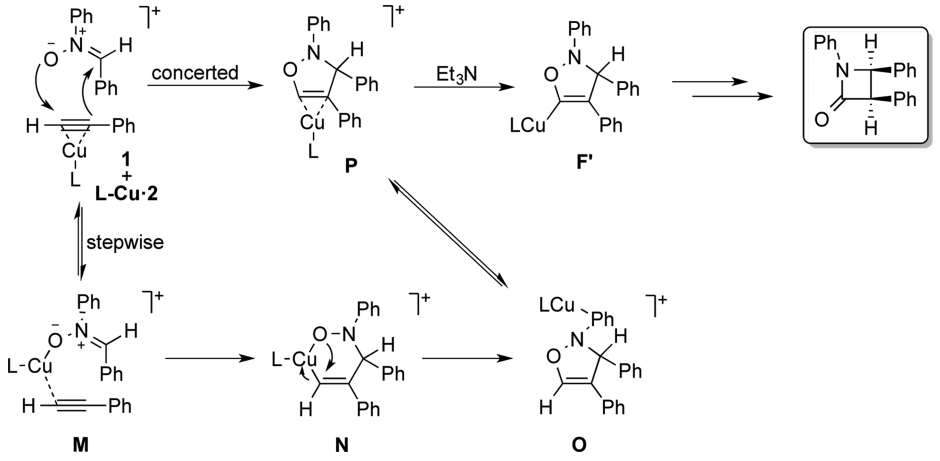

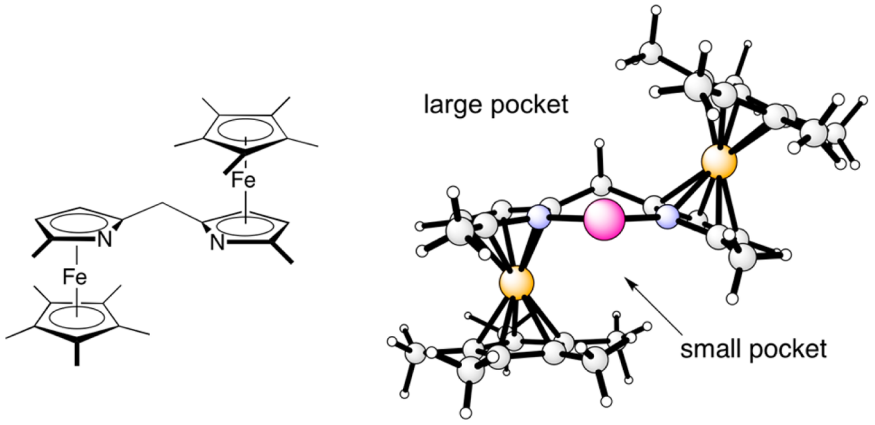

Figure 6. Schematic drawing of the (*R*,*R*)-bis(azaferrocene) ligand and optimized structure of its complex with copper.

step is found to be 22.4 kcal/mol, which is the lowest among the three possibilities considered within this mechanistic scenario. This step is moreover irreversible, which means that the predominant formation of the unproductive isoxazoline **Q** should be expected. Thus, the facts that the mechanism with no initial alkyne deprotonation has significantly higher energy barriers compared with the one involving two copper ions, and that it is unable to reproduce the outcome of the Kinugasa reaction make this mechanism unlikely for the nonchiral ligand.

To summarize this section, from the overall analysis of the mechanisms investigated here with phenanthroline as a ligand, it is clear that the most reasonable one in terms of energies is the mechanism involving an initial deprotonation of the alkyne and a cycloaddition assisted by two copper ions (Figure 2 and Scheme 4). The two other mechanistic possibilities considered here have higher energy barriers (see free energy profiles in Figures 4 and 5).

3.3. Enantioselective Reaction with Bis(azaferrocene) Ligand. Having discussed the mechanism using phenanthroline as the ligand, we now focus on the enantioselective reaction. We consider the reaction between *N*,*α*-diphenyl nitrone **1** and phenyl acetylene **2** using the full (*R*,*R*)-bis(azaferrocene) ligand employed in the experimental study (Figure 6).[7] In this case, the product was obtained in 95:5 dr, in favor of the *cis* diastereoisomer, and with a 77% ee for the major diastereoisomer, favoring the (*R*,*R*)-enantiomer.[7] Before discussing the results, it is important to note that, due to the presence of a methylenic carbon connecting the two azaferrocene moieties, when the ligand is bound to the metal the complex is not C_2-symmetric. It has namely two pockets of different sizes (see Figure 6), and this has consequences for the number of transition states that have to be located, since the orientation of the reactants in the two pockets will not be equivalent.

Significant differences can arise in the energies of the various mechanisms when using the large chiral ligand compared to phenanthroline, especially when comparing the mechanism with two copper ions with those with only one copper involved. Therefore, all mechanisms considered for the smaller ligand were also calculated for the enantioselective reaction.

In general, reaction barriers were found to be significantly higher with the chiral ligand compared to those with phenanthroline, with the highest increase observed for the mechanism involving two copper ions. However, despite the great difference in size between the ligands, the energetics of the deprotonation of the alkyne were found to be quite similar. Namely, in the presence of one copper ion with bis(azaferrocene) ligand, the deprotonation was found to be endergonic by 15.3 kcal/mol (9.2 kcal/mol with phenanthroline), while the deprotonation leading to the dicopper-acetylide was found to be exergonic by 1.8 kcal/mol (3.3 kcal/mol with phenanthroline).

The calculated free energy profile for the mechanism involving the initial deprotonation of the alkyne with two copper ions is shown in Figure 7 and the optimized structures of selected intermediates and lowest-energy TSs are shown in Figure 8.[25] Interestingly, it was found that, when the nitrone coordinates one of the copper ions of the dicopper-acetylide,

DOI: 10.1021/jo502838p
J. Org. Chem. 2015, 80, 2649−2660

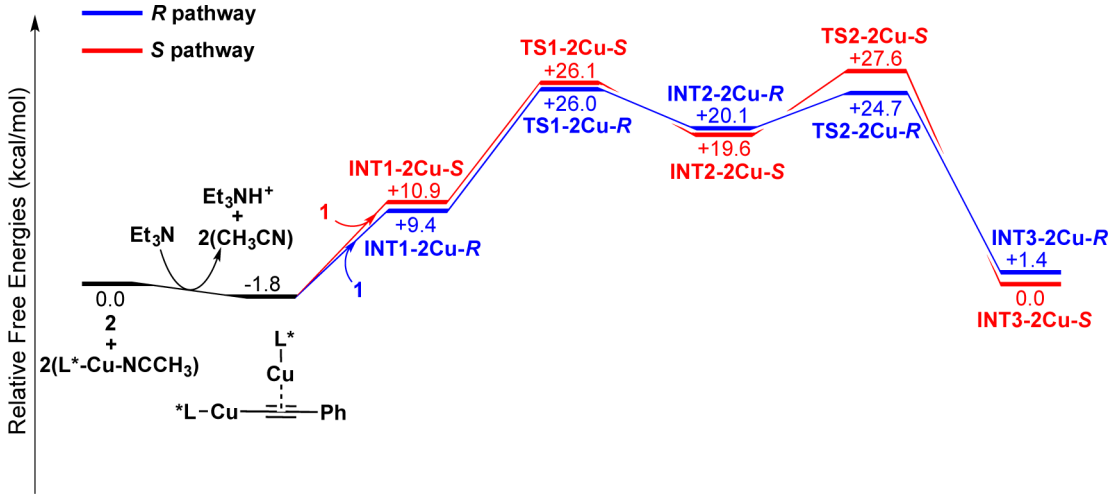

Figure 7. Free energy profile for the enantioselective stepwise cycloaddition involving two copper ions.

the ligand on the same copper ion becomes monodentate (see, for example, **INT1-2Cu-*R*** in Figure 8). As a consequence, the coordination of the nitrone is endergonic by ca. 11 kcal/mol, while the same step in the mechanism with the phenanthroline ligand was found to be exergonic by 0.3 kcal/mol. Next, the transition states for the stepwise formation of the five-membered ring intermediate, analogous to **E**, were optimized. Several alternatives are possible for each transition state and intermediate, depending mainly on which of the nitrone prochiral faces is attacked by the alkynyl group (thus determining the final stereochemistry of the product), on the relative orientation of the two ligands, and on the rotation of the dissociated azaferrocene moiety. All possible orientations and rotamers were calculated, but here we will present and discuss only those associated with the lowest energy barriers (see Figures 7 and 8). The reaction follows the same mechanism as with phenanthroline, with a C−C bond formation affording the six-membered ring intermediate, followed by a ring contraction resulting in the formation of the metalated isoxazoline. The calculated reaction barriers are significantly higher than those with phenanthroline (ca. 28 vs 16 kcal/mol), which is consistent with the experimental observation of the enantioselective reaction being very slow.[7] This difference is largely due to the endergonic rearrangement of one of the copper ligands when the nitrone binds to copper (i.e., the formation of **INT1-2Cu-*R*** or **INT1-2Cu-*S***, see Figure 7).

The pathway leading to the formation of the *R* isomer is favored by 1.6 kcal/mol over the pathway leading to the formation of the *S* isomer (difference in energy between **TS1-2Cu-*R*** and **TS2-2Cu-*S***). This is in good agreement with the experimental value of 77% ee, which corresponds to an energy difference of 1.1 kcal/mol. While the barriers for the first C−C bond formation step are very close (difference of 0.1 kcal/mol, see Figure 7), the barriers for the ring contraction differ by 2.9 kcal/mol. The reason is that, in **TS2-2Cu-*S***, the phenyl group bound to the nitrogen points toward one of the azaferrocene moieties, leading to a steric clash not present in **TS2-2Cu-*R***.

Thus, according to these calculations, the mechanism involving two copper ions reproduces the experimentally observed enantioselectivity quite well. However, the absolute barrier is calculated to be 27.8 kcal/mol, which is comparable to the calculated barrier for the uncatalyzed reaction leading to the unproductive intermediate (27.5 kcal/mol, see Figure 1). Considering the error margin of the methods, the mechanism cannot be ruled out.

Every attempt to locate a transition state for a concerted cycloaddition occurring with the productive regiochemistry converged to the stepwise pathway. On the other hand, we could optimize a transition state for the first step of a stepwise cycloaddition occurring with the nonproductive regiochemistry, and the calculated barrier for this possibility was very high (34.7 kcal/mol relative to the isolated reactants, not shown in the free energy profile).

Next, we modeled the mechanism involving the initial deprotonation of the terminal alkyne with only one copper ion, analogous to the mechanism reported in Figure 4. The calculated free energy profile for this mechanism is shown in Figure 9 and the optimized structures are reported in the Supporting Information. As mentioned above, the deprotonation of the alkyne in the presence of one copper ion is endergonic by 15.3 kcal/mol. We found that after the formation of the copper-acetylide, the lowest-energy pathway leading to the formation of the *R* product is a stepwise mechanism (through **TS1$_d$-1Cu-*R*** and **TS2$_d$-1Cu-*R***), very similar to the one found for the reaction occurring with phenanthroline. Also in this case, the initial formation of a Cu(III) six-membered ring intermediate (**INT1$_d$-1Cu-*R***) is followed by a reductive elimination affording a metalated isoxazoline. The lowest-energy transition state affording the *S* product (**TS1$_d$-1Cu-*S***) also resembles the first step of a stepwise mechanism, i.e. the carbon−carbon bond formation leading to a six-membered ring intermediate. However, in this case, the ring contraction (corresponding to **TS$_{K-F}$** in the mechanism with phenanthroline or to **TS2$_d$-1Cu-*R*** in the mechanism leading to the *R* product) occurs without a barrier, and the reaction can be considered concerted.

When taking into account the deprotonation of the alkyne, the barriers for this mechanistic scenario are prohibitively high (36.3 and 40.6 kcal/mol for the *S* and *R* enantiomers, respectively). Moreover, the formation of the *S* product was found to be favored over the *R* one by 4.3 kcal/mol, in disagreement with the experimental results. Additionally, the TS for a concerted cycloaddition affording the nonproductive five-membered ring intermediate was found to have similar barrier (36.1 kcal/mol, not shown in the free energy profile) to the TS leading to the *S* enantiomer. On the basis of these results, the

DOI: 10.1021/jo502838p
J. Org. Chem. 2015, 80, 2649−2660

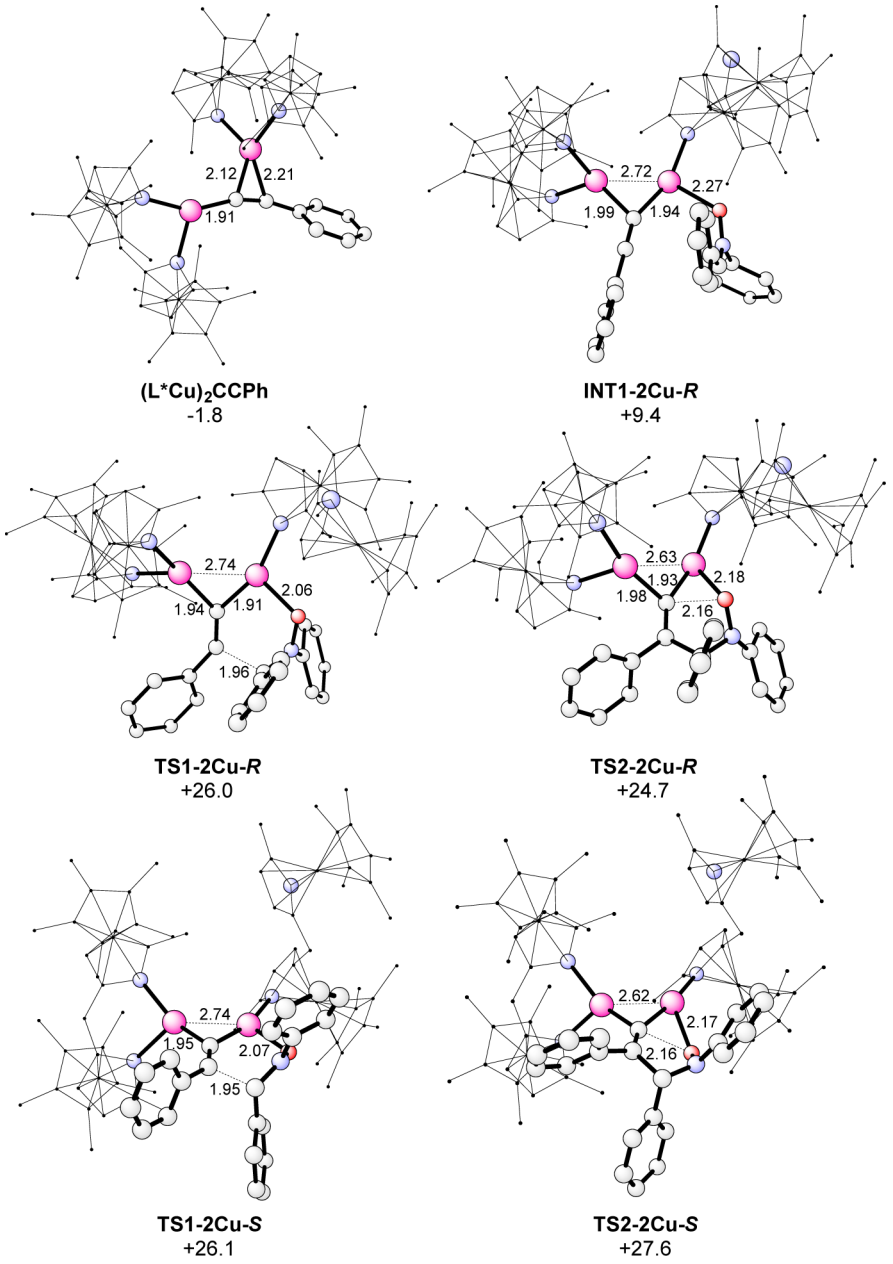

Figure 8. Selected optimized structures for the mechanism involving two Cu ions. Hydrogen atoms are omitted for clarity. Energies relative to the isolated reactants are given in kcal/mol (see Figure 7 for full energy profile).

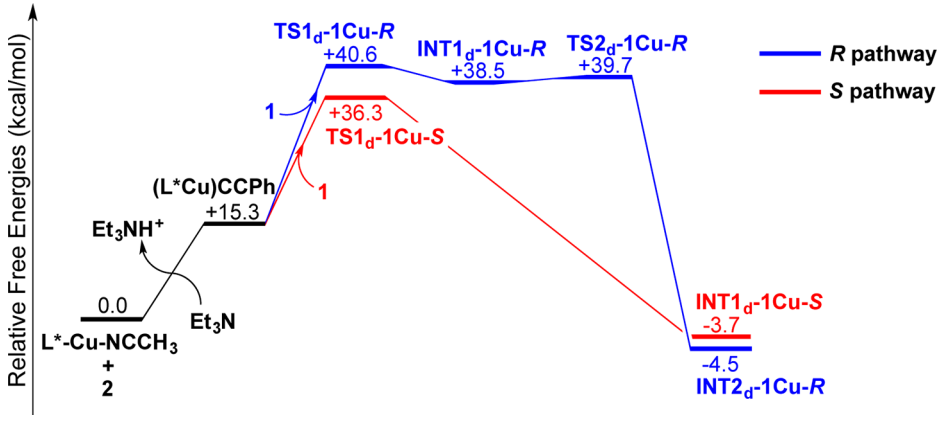

Figure 9. Free energy profile for the enantioselective reaction involving the deprotonation of the alkyne in the presence of one copper ion as the initial step.

DOI: 10.1021/jo502838p
J. Org. Chem. 2015, 80, 2649−2660

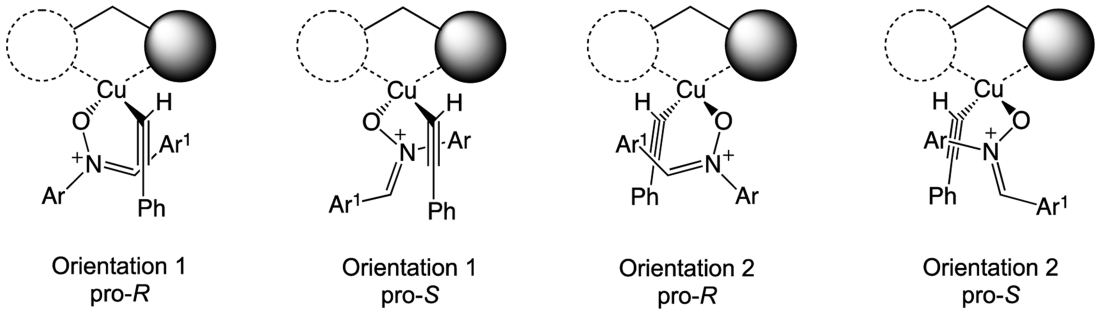

Figure 10. Possible orientations of the substrates in the ligand pockets, leading to the two isomeric intermediates. The large and small pockets are above and below the plane of the paper, respectively. The two spheres represent the azaferrocene moieties pointing out or in the plane of the paper (solid or dashed circles, respectively).

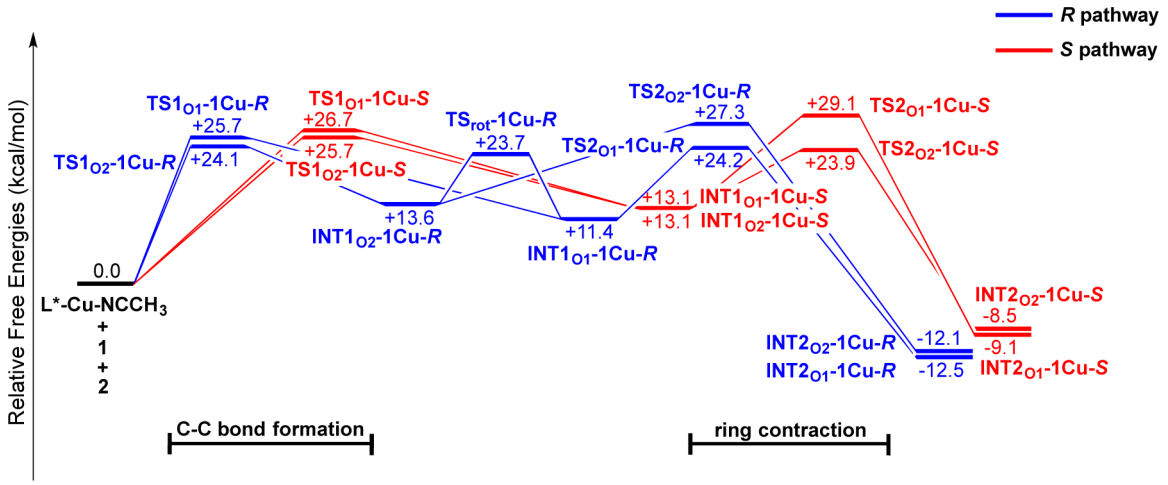

Figure 11. Free energy profile for the enantioselective stepwise cycloaddition not involving the initial deprotonation of the alkyne.

possibility of the enantioselective reaction occurring through this mechanism can be ruled out.

As a final option, we also modeled the formal cycloaddition steps for the reaction mechanism without the initial deprotonation of the alkyne, analogously to the mechanism reported in Figure 5 and Scheme 5 for phenanthroline. Here, there are four possibilities for the stepwise mechanism (see Figure 10). Namely, the nitrone and the alkyne can approach each other with the nitrone occupying the small pocket and the alkyne occupying the large pocket (called orientation 1), or *vice versa* (orientation 2). In each case, depending on which of the prochiral faces of the nitrone is attacked by the alkyne, the two different enantiomeric products can be formed.

We have calculated the free energy profiles for all these possibilities and the results are given in Figure 11. First, it is interesting to note that the overall barriers for the mechanism with the large chiral ligand now are quite similar to those calculated for the mechanism with two copper ions (see Figure 7). In the case of phenanthroline, the mechanism involving deprotonation with two copper ions was much more favored compared to the mechanism with the parent alkyne (cf. Figures 2 and 5).

As discussed above, two orientations of the reactants in the catalyst pockets are possible for each of the enantiomers. However, when analyzing the obtained energies for the formation of the two stereoisomers, it should be considered that after the first C−C bond formation transition state, analogous to $\mathbf{TS_{M\text{-}N}}$, the Cu(III) 6-membered ring intermediate (analogous to **N**) can rotate inside the ligand and adopt the opposite orientation, before undergoing the ring contraction through the second TS (analogue of $\mathbf{TS_{N-O}}$). This rotation does not affect the stereochemistry of the final product.

In the pathway leading to the *R* enantiomer, the lowest energy transition state for the C−C bond formation derives from "orientation 2" ($\mathbf{TS1_{O2}}$**-1Cu-*R***), while the lowest-energy transition state for the ring contraction ($\mathbf{TS2_{O1}}$**-1Cu-*R***) derives from "orientation 1". If a rotation occurs in the 6-membered ring intermediate, with $\mathbf{INT1_{O2}}$**-1Cu-*R*** converting to $\mathbf{INT1_{O1}}$**-1Cu-*R*** through $\mathbf{TS_{rot}}$**-1Cu-*R***, the overall barrier for the formation of the *R* product is 24.2 kcal/mol. In the pathway leading to the *S* enantiomer, the lowest-energy transition states for both steps follow "orientation 2", which means that no rotation of the 6-membered ring intermediate is necessary. The overall barrier for the formation of the *S* products is 25.7, corresponding to $\mathbf{TS1_{O2}}$**-1Cu-*S***. Thus, in this mechanism, the formation of the *R*-enantiomer is favored over the formation of the *S*-enantiomer by 1.5 kcal/mol, which is also in good agreement with the experimentally observed enantioselectivity.

The difference stems mostly from the initial C−C bond forming transition state. Inspection of the optimized geometries of $\mathbf{TS1_{O2}}$**-1Cu-*S*** and $\mathbf{TS1_{O2}}$**-1Cu-*R*** (Figure 12) reveals that in $\mathbf{TS1_{O2}}$**-1Cu-*R*** the phenyl group on the nitrone carbon points toward the relatively open upper-left quadrant (according to the orientation in Figure 10), whereas the phenyl on the nitrone nitrogen points toward the bulky ligand in the upper-right quadrant. In $\mathbf{TS1_{O2}}$**-1Cu-*S***, the pattern is the opposite, with the phenyl group on the nitrone nitrogen occupying a free

DOI: 10.1021/jo502838p
J. Org. Chem. 2015, 80, 2649−2660

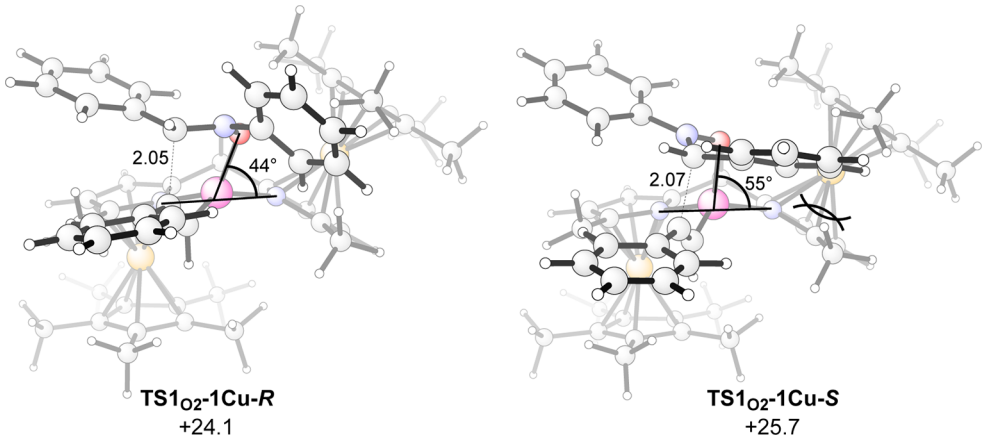

Figure 12. Lowest energy barrier transition states for the first C−C bond formation leading to the two enantiomeric products.

space and the phenyl on the nitrone carbon pointing toward the bulky group in the upper-right quadrant.

The phenyl on the nitrogen is relatively free to rotate to reduce steric repulsion in **TS1$_{O2}$-1Cu-*R***. On the other hand, the phenyl on the nitrone carbon, which is the carbon forming the bond to the alkyne, is more constrained, and the steric repulsion between this phenyl and the bulky azaferrocene group in the upper-right quadrant results in a displacement of the whole nitrone in **TS1$_{O2}$-1Cu-*S***. This can be seen from a comparison of the dihedral angles defined by the two nitrogens of the ligand, the copper ion and the oxygen of the nitrone. This angle is 44° in **TS1$_{O2}$-1Cu-*R*** and 55° in **TS1$_{O2}$-1Cu-*S***. The same angle is ca. 20° in the analogous transition state calculated for phenanthroline (**TS$_{M\text{-}N}$**), where the steric hindrance of the ligand is considerably less than in the chiral (bis)azaferrocene ligand.

Concerted transition states analogues to **TS$_{1+2\text{-}P}$** were found to be consistently higher in energy compared to the stepwise mechanisms. The barriers were calculated to be 29.8 and 32.3 kcal/mol for the TSs leading to the *R* and the *S* enantiomers, respectively. This is in contrast to the phenanthroline case, where the concerted and the stepwise pathways have quite similar barriers. Very importantly, the barriers for the concerted cycloaddition leading to the nonproductive isomeric isoxazoline (analogues to **TS$_{1+2\text{-}Q}$**) were also found to be higher in energy than those calculated for the stepwise mechanism, the lowest one being 27.7 kcal/mol.

To summarize this section, the mechanism involving the cycloaddition on the parent alkyne has an overall barrier that is quite close to the one of the mechanism with an initial deprotonation with two copper ions (24.2 and 27.8 kcal/mol, respectively). Both possibilities reproduce the experimentally observed enantioselectivity quite well. Considering the limitations of the computational methodology, it is therefore not possible on the basis of the current calculations to rule out any of them. On the other hand, the mechanism involving the initial deprotonation of the alkyne with one copper ion can be ruled out because of its high-energy barriers and its failure to reproduce the experimentally observed enantioselectivity.

4. CONCLUSIONS

In the present work, the mechanism and enantioselectivity of a catalytic Kinugasa reaction have been investigated by means of DFT calculations. Calculations performed with phenanthroline as a ligand establish that the mechanism involves two equivalents of copper, similarly to what has been suggested for the Cu(I)-catalyzed azide−alkyne cycloaddition.[21] In this mechanism, the copper promotes the initial deprotonation of the terminal alkyne to give a dicopper-acetylide, which then reacts with the nitrone in a stepwise manner to give a metalated isoxazoline intermediate. Subsequent protonation of the nitrogen of the 5-membered ring intermediate leads to the formation of a ketene, which can undergo a copper-catalyzed cyclization to give a 4-membered ring intermediate. Finally, tautomerization of this intermediate affords then the *β*-lactam product. This mechanism has the lowest barriers compared to the possible alternatives investigated in the current study.

On the other hand, for the enantioselective reaction using the large bis(azaferrocene) ligand, it was found that the mechanism proposed for the smaller model has higher absolute energy barriers. Moreover, these barriers are similar to those found for an alternative mechanism, involving the initial cycloaddition occurring in a stepwise manner on the parent alkyne. In this mechanism, the deprotonation essential for the formation of the metalated isoxazoline occurs at a later stage. Both mechanisms reproduce quite well the experimentally observed enantioselectivity, which can be rationalized on the basis of the steric repulsion between the ligand and the nitrone. It is not possible to rule out any of these possibilities based on the current calculations.

As a final note, it should be emphasized that according to the current calculations, the energetics of the various mechanistic possibilities can be quite sensitive to the nature of the ligand, something that should be taken into account when extending the conclusions to other catalytic conditions.

■ ASSOCIATED CONTENT

Supporting Information

Additional optimized structures and Cartesian coordinates of all stationary points. This material is available free of charge via the Internet at http://pubs.acs.org.

■ AUTHOR INFORMATION

Corresponding Author

*E-mail: himo@organ.su.se

Present Address

[†](S.S.) Department of Chemistry, Biology and Biotechnology, University of Perugia, Via Elce di Sotto 8, 06123 Perugia, Italy.

Notes

The authors declare no competing financial interest.

DOI: 10.1021/jo502838p
J. Org. Chem. 2015, 80, 2649−2660

■ ACKNOWLEDGMENTS

This work was supported by the Swedish Research Council, the Göran Gustafsson and Knut and Alice Wallenberg Foundations. Computer time was generously provided by the Swedish National Infrastructure for Computing.

■ REFERENCES

(1) For recent reviews, see: (a) Llarrull, L. I.; Testero, S. A.; Fisher, J. F.; Mobashery, S. *Curr. Opin. Microbiol.* **2010**, *13*, 551−557. (b) Kong, K. F.; Schneper, L.; Mathee, K. *APMIS* **2010**, *118*, 1−36. (c) Shahid, M.; Sobia, F.; Singh, A.; Malik, A.; Khan, H. M.; Jonas, D.; Hawkey, P. M. *Crit. Rev. Microbiol.* **2009**, *35*, 81−108.

(2) For selected reviews, see: (a) D'hooghe, M.; Dekeukeleire, S.; Leemans, E.; De Kimpe, N. *Pure. Appl. Chem.* **2010**, *82*, 1749−1759. (b) Alcaide, B.; Almendros, P.; Aragoncillo, C. *Chem. Rev.* **2007**, *107*, 4437−4492. (c) Ojima, I.; Delaloge, F. *Chem. Soc. Rev.* **1997**, *26*, 377−386.

(3) For reviews, see: (a) Allen, A. D.; Tidwell, T. T. *Eur. J. Org. Chem.* **2012**, 1081−1096. (b) Aranda, M. T.; Perez-Faginas, P.; Gonzalez-Muniz, R. *Curr. Org. Synth.* **2009**, *6*, 325−341. (c) Fu, N.; Tidwell, T. T. *Tetrahedron* **2008**, *64*, 10465−10496. (d) France, S.; Weatherwax, A.; Taggi, A. E.; Lectka, T. *Acc. Chem. Res.* **2004**, *37*, 592−600. (e) Palomo, C.; Aizpurua, J. M.; Ganboa, I.; Oiarbide, M. *Curr. Med. Chem.* **2004**, *11*, 1837−1872. (f) Palomo, C.; Aizpurua, J. M.; Ganboa, I.; Oiarbide, M. *Eur. J. Org. Chem.* **1999**, 3223−3235.

(4) For reviews, see: (a) Mandal, B.; Basu, B. *Top. Heterocycl. Chem.* **2013**, *30*, 85−110. (b) Pal, R.; Ghosh, S. C.; Chandra, K.; Basak, A. *Synlett* **2007**, 2321−2330. (c) Marco-Contelles, J. *Angew. Chem., Int. Ed.* **2004**, *43*, 2198−2200. (d) Khangarot, R. K.; Kaliappan, K. P. *Eur. J. Org. Chem.* **2013**, 7664−7677. (e) Stecko, S.; Furman, B.; Chmielewski, M. *Tetrahedron* **2014**, *70*, 7817−7844.

(5) Kinugasa, M.; Hashimoto, S. *J. Chem. Soc., Chem. Commun.* **1972**, 466−467.

(6) (a) Okuro, K.; Enna, M.; Miura, M.; Nomura, M. *J. Chem. Soc., Chem. Commun.* **1993**, 1107−1108. (b) Miura, M.; Enna, M.; Okuro, K.; Nomura, M. *J. Org. Chem.* **1995**, *60*, 4999−5004.

(7) Lo, M. M.-C.; Fu, G. C. *J. Am. Chem. Soc.* **2002**, *124*, 4572−4573.

(8) Shintani, R.; Fu, G. C. *Angew. Chem., Int. Ed.* **2003**, *42*, 4082−4085.

(9) (a) Chen, J.-H.; Liao, S.-H.; Sun, X.-L.; Shen, Q.; Tang, Y. *Tetrahedron* **2012**, *68*, 5042−5045. (b) Saito, T.; Kikuchi, T.; Tanabe, H.; Yahiro, J.; Otani, T. *Tetrahedron Lett.* **2009**, *50*, 4969−4972. (c) Coyne, A. G.; Müller-Bunz, H.; Guiry, P. J. *Tetrahedron: Asymmetry* **2007**, *18*, 199−207. (d) Ye, M. C.; Zhou, J.; Tang, Y. *J. Org. Chem.* **2006**, *71*, 3576−3582. (e) Basak, A.; Ghosh, S. C. *Synlett* **2004**, 1637−1639. (f) Ye, M.-C.; Zhou, J.; Huang, Z.-Z.; Tang, Y. *Chem. Commun.* **2003**, 2554−2555. (g) Chen, Z.; Lin, L.; Wang, M.; Liu, X.; Feng, X. *Chem.—Eur. J.* **2013**, *19*, 7561−7567.

(10) Ding, L. K.; Irwin, W. J. *J. Chem. Soc., Perkin Trans. 1* **1976**, 2382−2386.

(11) Ahn, C.; Kennington, J. W.; DeShong, P. *J. Org. Chem.* **1994**, *59*, 6282−6286.

(12) (a) Becke, A. D. *J. Chem. Phys.* **1993**, *98*, 5648−5652. (b) Lee, C.; Yang, W.; Parr, R. G. *Phys. Rev.* **1988**, *B37*, 785−789.

(13) *Gaussian 03*, Revision D.01; Frisch, M. J.; Trucks, G. W.; Schlegel, H. B.; Scuseria, G. E.; Robb, M. A.; Cheeseman, J. R.; Montgomery, Jr., J. A.; Vreven, T.; Kudin, K. N.; Burant, J. C.; Millam, J. M.; Iyengar, S. S.; Tomasi, J.; Barone, V.; Mennucci, B.; Cossi, M.; Scalmani, G.; Rega, N.; Petersson, G. A.; Nakatsuji, H.; Hada, M.; Ehara, M.; Toyota, K.; Fukuda, R.; Hasegawa, J.; Ishida, M.; Nakajima, T.; Honda, Y.; Kitao, O.; Nakai, H.; Klene, M.; Li, X.; Knox, J. E.; Hratchian, H. P.; Cross, J. B.; Bakken, V.; Adamo, C.; Jaramillo, J.; Gomperts, R.; Stratmann, R. E.; Yazyev, O.; Austin, A. J.; Cammi, R.; Pomelli, C.; Ochterski, J. W.; Ayala, P. Y.; Morokuma, K.; Voth, G. A.; Salvador, P.; Dannenberg, J. J.; Zakrzewski, V. G.; Dapprich, S.; Daniels, A. D.; Strain, M. C.; Farkas, O.; Malick, D. K.; Rabuck, A. D.; Raghavachari, K.; Foresman, J. B.; Ortiz, J. V.; Cui, Q.; Baboul, A. G.; Clifford, S.; Cioslowski, J.; Stefanov, B. B.; Liu, G.; Liashenko, A.; Piskorz, P.; Komaromi, I.; Martin, R. L.; Fox, D. J.; Keith, T.; Al-Laham, M. A.; Peng, C. Y.; Nanayakkara, A.; Challacombe, M.; Gill, P. M. W.; Johnson, B.; Chen, W.; Wong, M. W.; Gonzalez, C.; Pople, J. A.; Gaussian, Inc.: Wallingford, CT, 2004.

(14) Hay, P. J.; Wadt, W. R. *J. Chem. Phys.* **1985**, *82*, 270−283.

(15) (a) Gonzalez, C.; Schlegel, H. B. *J. Chem. Phys.* **1989**, *90*, 2154−2161. (b) Gonzalez, C.; Schlegel, H. B. *J. Phys. Chem.* **1990**, *94*, 5523−5527.

(16) (a) Klamt, A.; Schüürmann, G. *J. Chem. Soc., Perkin Trans. 2* **1993**, 799−805. (b) Andzelm, J.; Kölmel, C.; Klamt, A. *J. Chem. Phys.* **1995**, *103*, 9312−9320. (c) Barone, V.; Cossi, M. *J. Phys. Chem. A* **1998**, *102*, 1995−2001. (d) Cossi, M.; Rega, N.; Scalmani, G.; Barone, V. *J. Comput. Chem.* **2003**, *24*, 669−691.

(17) Grimme, S. *J. Comput. Chem.* **2006**, *27*, 1787−1799.

(18) For examples, see: (a) Minenkov, Y.; Occhipinti, G.; Jensen, V. R. *J. Phys. Chem. A* **2009**, *113*, 11833−11844. (b) Siegbahn, P. E. M.; Blomberg, M. R. A.; Chen, S.-L. *J. Chem. Theory Comput.* **2010**, *6*, 2040−2044. (c) Harvey, J. N. *Faraday Discuss.* **2010**, *145*, 487−505. (d) McMullin, C. L.; Jover, J.; Harvey, J. N.; Fey, N. *Dalton Trans.* **2010**, *39*, 10833−10836. (e) Lonsdale, R.; Harvey, J. N.; Mulholland, A. J. *J. Phys. Chem. Lett.* **2010**, *1*, 3232−3237. (f) Osuna, S.; Swart, M.; Solà, M. *J. Phys. Chem. A* **2011**, *115*, 3491−3496. (g) Ahlquist, M. S. G.; Norrby, P.-O. *Angew. Chem., Int. Ed.* **2011**, *50*, 11794−11797. (h) Santoro, S.; Liao, R.-Z.; Himo, F. *J. Org. Chem.* **2011**, *76*, 9246−9252. (i) Xu, X.; Liu, P.; Lesser, A.; Sirois, L. E.; Wender, P. A.; Houk, K. N. *J. Am. Chem. Soc.* **2012**, *134*, 11012−11025.

(19) Himo, F.; Lovell, T.; Hilgraf, R.; Rostovtsev, V. V.; Noodleman, L.; Sharpless, K. B.; Fokin, V. V. *J. Am. Chem. Soc.* **2005**, *127*, 210−216.

(20) Fu and co-workers used *N*,*N*-dicyclohexylmethylamine as the base (see ref 7). Triethylamine is a good model of this.

(21) (a) Rodionov, V. O.; Fokin, V. V.; Finn, M. G. *Angew. Chem., Int. Ed.* **2005**, *44*, 2210−2215. (b) Rodionov, V. O.; Presolski, S. I.; Díaz, D. D.; Fokin, V. V.; Finn, M. G. *J. Am. Chem. Soc.* **2007**, *129*, 12705−12712. (c) Straub, B. F. *Chem. Commun.* **2007**, 3868−3870. (d) Ahlquist, M.; Fokin, V. V. *Organometallics* **2007**, *26*, 4389−4391. (e) Kuang, G.-C.; Guha, P. M.; Brotherton, W. S.; Simmons, J. T.; Stankee, L. A.; Nguyen, B. T.; Clark, R. J.; Zhu, L. *J. Am. Chem. Soc.* **2011**, *133*, 13984−14001. (f) Worrell, B. T.; Malik, J. A.; Fokin, V. V. *Science* **2013**, *340*, 457−460.

(22) Kinetically, deprotonation of alkynes in the presence of copper and a base is known to be a fast process, see for example: (a) Shi, W.; Luo, Y.; Luo, X.; Chao, L.; Zhang, H.; Wang, J.; Lei, A. *J. Am. Chem. Soc.* **2008**, *130*, 14713−14720. (b) Shao, C.; Cheng, G.; Su, D.; Xu, J.; Wang, X.; Hu, Y. *Adv. Synth. Catal.* **2010**, *352*, 1587−1592. (c) Jarosz, P.; Thall, J.; Schneider, J.; Kumaresan, D.; Schmehl, R.; Eisenberg, R. *Energy Environ. Sci.* **2008**, *1*, 573−583. (d) Castro, C. E.; Gaughan, E. J.; Owsley, D. C. *J. Org. Chem.* **1966**, *31*, 4071−4078. (e) Hein, J. E.; Fokin, V. V. *Chem. Soc. Rev.* **2010**, *39*, 1302−1315. We have explicitly calculated a possible pathway for deprotonation with two copper ions and using triethylamine as a base, and the overall barrier was found to be only ca 10 kcal/mol relative to the reactants. See Supporting Information for details.

(23) Optimizing the geometry of the cyclic enolate **I** after removal of the LCu^+ moiety results in the ring opening.

(24) **F′** is the equivalent of intermediate **F** presented in the first mechanism. The difference is that in **F′**, the Et_3NH^+ resulting from the deprotonation of the ring is included in the supercomplex.

(25) In the reaction with phenanthroline, the L-Cu·**2** complex was set as the reference state, while in the reaction with the chiral ligand, this is represented by the L*-Cu-$NCCCH_3$ complex. The reason for this is that LCu^+ (L = phenanthroline) favors the coordination to phenyl acetylene over acetonitrile by 1.5 kcal/mol, while L^*Cu^+ (L* = (*R*,*R*)-bis(azaferrocene)) favors the coordination to acetonitrile over phenyl acetylene by 2.4 kcal/mol.

DOI: 10.1021/jo502838p
J. Org. Chem. 2015, 80, 2649−2660